Creating the conditions of anomalous self-diffusion in a liquid with molecular dynamics



J. Stat. Mech. (2010) P04004

(http://iopscience.iop.org/1742-5468/2010/04/P04004)

Journal of Statistical Mechanics: Theory and Experiment
An IOP and SISSA journal

# Creating the conditions of anomalous self-diffusion in a liquid with molecular dynamics

**Simon Standaert, Jan Ryckebusch and Lesley De Cruz**

Department of Physics and Astronomy, Ghent University, Proeftuinstraat 86, B-9000 Gent, Belgium
E-mail: simon.standaert@ugent.be, jan.ryckebusch@ugent.be and lesley.decruz@ugent.be

Received 15 December 2009
Accepted 5 March 2010
Published 1 April 2010

Online at stacks.iop.org/JSTAT/2010/P04004
doi:10.1088/1742-5468/2010/04/P04004

**Abstract.** We propose a computational method for simulating anomalous self-diffusion in a simple liquid. The method is based on a molecular dynamics simulation on which we impose the following two conditions: firstly, the inter-particle interaction is described using a soft-core potential; and secondly, the system is forced out of equilibrium. The latter can be achieved by subjecting the system to changes in the length scale, intermittently. In many respects, our simulation system bears a resemblance to slowly driven sandpile models displaying self-organized criticality. We find non-Gaussian single-time-step displacement distributions during the out-of-equilibrium time periods of the simulation.

**Keywords:** driven diffusive systems (theory), self-organized criticality (theory), diffusion, molecular dynamics

**ArXiv ePrint:** 0907.1856

J. Stat. Mech. (2010) P04004

## Contents



## 1. Introduction

Ever since Einstein made geometric Brownian motion famous [1], a simple liquid has been the prime example of a system in which normal diffusion occurs. Gaussian statistics, which characterizes normal diffusion, is extensively utilized in various fields of research. Anomalous, non-Gaussian diffusion is characterized by a probability distribution function with power-law tails $P(z > z_0) \sim |z|^{-\alpha}$. The limiting distribution of the sum of independent variables with this property is a Lévy distribution [2]–[4]. It is well known that anomalous diffusion, in the general sense, can occur in both equilibrium and non-equilibrium contexts [5, 6]. In equilibrium conditions, systems with persistent time correlations between the Gaussian step increments can generate anomalous self-diffusion [6]. Amongst the fields in which examples of non-Gaussian dynamics are found are economics [7]–[9], biology [10, 11] and solid state physics [12]. For example, the self-diffusion of small molecules in bulk amorphous polymers has been shown to display an anomalous regime [13].

The above observations have motivated extensive efforts to investigate the underlying mechanisms of non-Gaussian dynamics. There are numerous methods for achieving anomalous diffusion in lower-dimensional systems [14], in media [15, 16], in networks [17] and in turbulence [18]. To our knowledge, however, in the literature there is no mention of a simple computational method for achieving conditions of anomalous self-diffusion in a 3D liquid. Here, we wish to propose such a method. We present a robust technique for altering the dynamics of a molecular dynamics (MD) simulation of a simple liquid in such a manner that anomalous self-diffusion emerges. These anomalous properties emerge in the one-dimensional single-time-step displacement distributions $P(\Delta x)$. In particular, we propose to combine a MD simulation technique with a soft-core inter-particle potential and out-of-equilibrium conditions.

MD is a very powerful simulation technique that is based on (numerically) solving the equations of motion for many interacting particles at carefully chosen regular time intervals. As a consequence, a MD simulation allows one to investigate many aspects of liquids and other systems such as self-diffusion, phase diagrams, the absorption of particles and viscosity [19]–[22]. It is well known that in classical MD simulations with a Lennard-Jones (LJ) inter-particle potential, the mean square displacement (MSD) $\langle \Delta r^2(t) \rangle$ has a linear time dependence, and that $P(\Delta x)$ is a Gaussian distribution.

doi:10.1088/1742-5468/2010/04/P04004


J. Stat. Mech. (2010) P04004

**Table 1.** Fitted parameters for the soft-core potential for five different values of $H$.

| $H$ (in units $U_A$) | 5 | 10 | 20 | 50 | 200 |
|---|---|---|---|---|---|
| $\Delta$ (in units $R_A^{-1}$) | 36.7 | 31.9 | 39.4 | 26.0 | 28.3 |
| $U_A$ (in units $U_A$) | 1 | 1 | 1 | 1 | 1 |
| $2\delta_A^2$ (in units $R_A^2$) | 0.089 | 0.090 | 0.062 | 0.096 | 0.089 |
| $R_A$ (in units $R_A$) | 1 | 1 | 1 | 1 | 1 |
| $R_R$ (in units $R_A$) | 0.85 | 0.82 | 0.79 | 0.73 | 0.70 |

## 2. Formalism

When attempting to create conditions under which anomalous self-diffusion emerges, the hard core of the LJ potential, $U_{\rm LJ}(r) = \epsilon((r_0/r)^{12} - 2(r_0/r)^6)$, poses a real challenge. Indeed, for a liquid with conditions of anomalous self-diffusion, $P(\Delta x)$ obtains heavy tails and the particles can occasionally traverse a relatively large distance during a single time step. In the MD simulations, those particles will momentarily travel with an exceptionally large speed. Due to the finite time resolution of the simulation, they can penetrate the hard core of the LJ potential and attain a velocity that is much larger than the average velocities in the simulation. This, in turn, dramatically increases the probability for particles entering the hard core of other particles and ignites a chain reaction that makes the simulation go out of control. In order to remedy this, we have renormalized the short-range part of the Lennard-Jones potential and used the following soft-core potential [23]:

$$U_{\rm SC}(r) = \frac{H}{1 + \exp \Delta(r - R_R)} - U_A \exp\left[-\frac{(r - R_A)^2}{2\delta_A^2}\right]. \quad (1)$$

$H$ determines the height of the potential barrier and below we will investigate the influence of this parameter. The parameters $\Delta, R_R, R_A, U_A, \delta_A$ were optimized so as to match the medium- and long-range parts of $U_{\rm LJ}(r)$ and are listed in table 1.

The inter-molecular interaction range $R_A$ determines the length scale in the system and we take $R_A = r_0 = 3.405 \times 10^{-10}$ m, the diameter of argon. The units adopted for energy and mass are also determined for a simulation that involves argon: mass units, $m = 6.63 \times 10^{-26}$ kg, and energy units, $E = U_A = 1.65 \times 10^{-21}$ J. All variables in this paper are expressed in terms of these units: lengths in units of $R_A$ and energies in units of $U_A$. The parameter $H$ determines the hardness of the core of the potential. The softer the core, the more penetrable the particles become.

First, we wish to discriminate between the dynamical properties of the monatomic liquid for $U_{\rm LJ}(r)$ and $U_{\rm SC}(r)$. To this end, the potential $U_{\rm SC}(r)$ of (1) is used in a classical MD simulation program. We investigate the self-diffusion properties, the velocity auto-correlation function (VACF) and the radial distribution function (RDF). The VACF tracks the persistence of the motion over time and the RDF provides information about the relative particle positions, providing a means of discriminating between the liquid, gaseous and solid phases. The thermodynamic properties, such as temperature, potential and kinetic energy, are also monitored. In order to solve the equations of motion, we

J. Stat. Mech. (2010) P04004

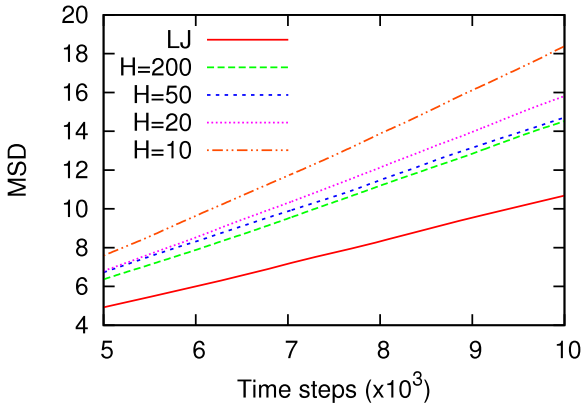


**Figure 1.** The MSD as a function of simulation time for different soft-core parameters $H$ and for a LJ potential. The simulation has an initial density of 0.5 and an initial temperature of 0.7. The density of the system is given in particles per unit of volume and the temperature is given in units of $(U_A/k_B)$, with $k_B = 1$. The simulations are performed with 8788 particles, and the time step is determined by $(0.001\rho^{-1/3}/\sqrt{2T})$.

adopt the Verlet algorithm, which is a symplectic integrator. We adopt periodic boundary conditions to avoid a disproportionate influence of surface effects. This means that our simulation system does not have walls.

Figure 1 shows the time dependence of the MSD for various values of $H$ of the soft-core potential and for a LJ potential. For large values of $H$, the soft-core potential of (1) is qualitatively similar to $U_{LJ}(r)$. For all values of $H$, the dynamics of the system leads to normal diffusion ($\langle \Delta r^2 \rangle \sim t$). The simulation results indicate that the diffusion coefficient $D$ ($\langle \Delta r^2 \rangle = 6Dt$) depends on the softness of the potential. The harder the short-range part is, the lower $D$ will be, as the collisions approach a hard-sphere interaction.

In [24] a region is identified in which a diffusion anomaly is found. This *anomalous diffusion region* in the $P$–$T$ phase diagram of a fluid is characterized by a diffusion coefficient that increases with the density. In this work we reserve the word anomalous uniquely for non-Gaussian displacement distributions and make no further reference to an atypical density and pressure dependence of the diffusion coefficient.

The qualitative features of the VACF, RDF, energy and temperature obtained with $U_{SC}(r)$ resemble those of a simulation with a LJ potential. There are some differences in the computed observables, and the RDF, for example, reflects that the soft core allows penetration. The positional structure, typical for a liquid, is still visible in the RDF. The most important aspect, however, is the ubiquitous presence of the Gaussian statistics in the self-diffusion properties.

In [25] it was shown that soft potentials with a finite height at the origin of the coordinates can display a so-called $H$-instability. The $H$-instability was observed to occur for certain combinations of the parameters in a generalized Morse potential. Our $U_{SC}(r)$ has a balanced amount of short-range repulsion and medium-range attraction. During all stages of the simulations we have monitored the RDFs. The RDFs obtained with $U_{SC}(r)$ display all characteristics of a typical liquid and we find no signatures of a collapse.



J. Stat. Mech. (2010) P04004

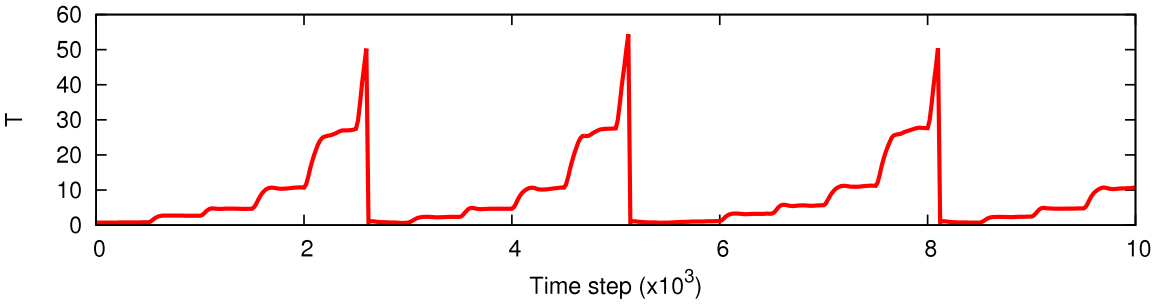


**Figure 2.** Temperature as a function of time for a simulation with a radial rescaling with $\lambda(t=0)=0.75$ and $\tau=500$. When the temperature reaches 50, the radii and the temperature are reset to their original values ($T_{\rm init}=0.7$).

## 3. Out-of-equilibrium simulation

We now turn to simulations under non-equilibrium conditions. Under equilibrium conditions, the energy is conserved and the temperature fluctuates mildly around a certain value. We introduce non-equilibrium conditions by driving the system and modifying the inter-particle interaction. This can be achieved by rescaling the radial distances in the soft-core interaction $U_{\rm SC}(r) \to U_{\rm SC}(\lambda(t)r)$ with $\lambda(t) \leq 1$. This is equivalent to an effective increase in the size of the molecules. During the simulation, we adopt a stepwise change in $\lambda(t)$ at regular intervals (the length of the intervals gets determined by the variable $\tau$). We use the protocol

$$\lambda(t) = [\lambda(t=0)]^{\lfloor (t/\tau) \rfloor}, \tag{2}$$

where $\lfloor (t/\tau) \rfloor$ rounds $(t/\tau)$ towards positive integer values ($\leq (t/\tau)$). The values for $\tau$ and $\lambda(t=0)$ are fixed at the start of the simulation. The two parameters $\tau$ and $\lambda(t=0)$ can also be made to vary during the simulation (e.g. by drawing them from a Gaussian distribution). We have verified that this does not lead to sizably different results and makes the subsequent analysis more convoluted. For the results shown here, we have adopted fixed values for $\tau$ and $\lambda(t=0)$.

The forced rescaling allows the dynamics of the system to be changed dramatically, because particles that were attracting each other end up repelling each other due to the driven change in the inter-particle interaction range. As the imposed changes in the inter-particle interactions occur under conditions of constant density, the system develops regions of high energy density. Through the dynamics of the system, local energy surplus dissipates into sizable kinetic energy and an increase in the temperature of the system is observed. Figure 2 shows the evolution of the temperature with time for a simulation that undergoes a rescaling of the soft-core interaction of the particles. It is clear that the driven change in the radius of the molecules has a large effect on the temperature. After rescaling the radial distances, it takes of the order of a few hundred time steps for the temperature to reach a new equilibrium value.

To illustrate the effect of the radial rescaling on the internal dynamics of the system, the potential energy fluctuation of the system during one simulation step is shown in figure 3. We consider results for $U_{\rm LJ}(r)$ and $U_{\rm SC}(r)$ under typical equilibrium conditions



J. Stat. Mech. (2010) P04004

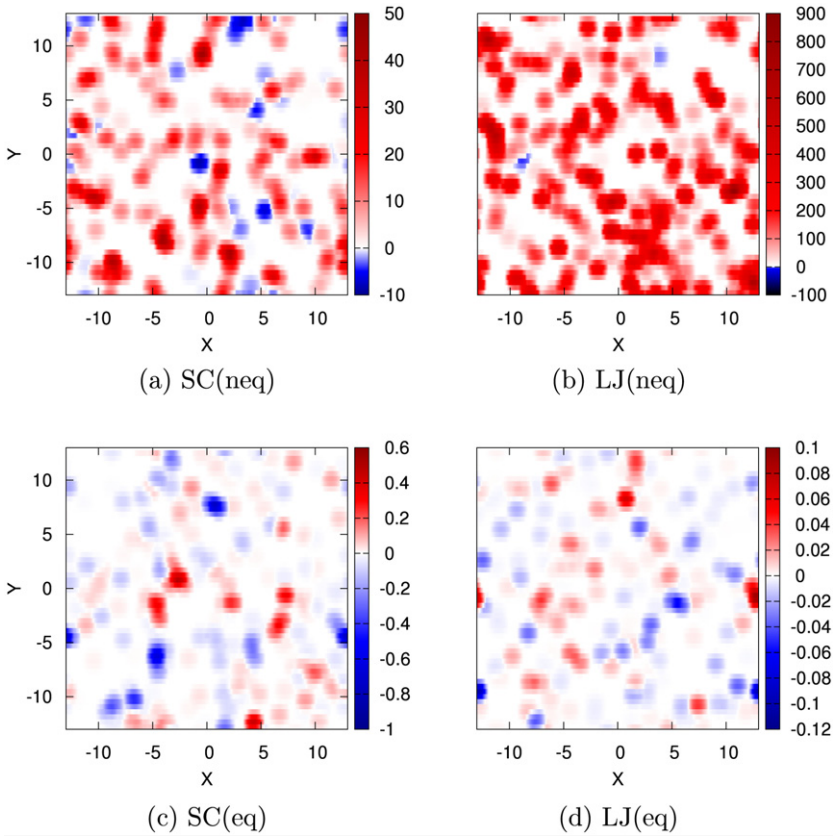


**Figure 3.** A typical spatial distribution of the potential energy changes $\Delta E_{\rm pot}(\boldsymbol{r}_i)$ in one time step. We show the projection onto the $xy$ plane for $|z_i| \leq 0.5$ under conditions of (a) a soft-core potential just after rescaling with $\lambda(t = 0) = 0.7$ (neq), (b) a LJ potential just after rescaling with $\lambda(t = 0) = 0.7$ (neq), (c) a soft-core potential during equilibrium (eq), (d) a LJ potential during equilibrium (eq).

and a situation just after a radial rescaling. For every particle the difference in potential energy with respect to the previous configuration is shown:

$$\Delta E_{\rm pot}(\mathbf{r}_i) = \sum_{j \neq i} U(\mathbf{r}_{ij}(t + \Delta t)) - U(\mathbf{r}_{ij}(t)). \tag{3}$$

The panels of figure 3 represent a projection of a slice ($\forall i$: $|z_i| \leq 0.5$) onto the $xy$ plane. Figure 3(a) indicates that through a sudden rescaling of the radial distances one creates regions in which the total amount of potential energy gain is much larger than the average value. Figure 3(b) shows that the hard core of $U_{\rm LJ}(r)$ results in values of $\Delta E_{\rm pot}$ as high as 800, whereas this is not seen in figure 3(a). With energy fluctuations of this size, the velocities of the particles attain values that are not compatible with a finite time step. Figures 3(c) and (d) show a similar type of projection for typical equilibrium conditions. The scale of $\Delta E_{\rm pot}$ is clearly much smaller than in the non-equilibrium situations of figures 3(a) and (b).

The regular rescaling of the inter-particle distances drives the system's thermodynamic properties such as the temperature and the energy away from equilibrium, i.e. mild



J. Stat. Mech. (2010) P04004

fluctuations around a constant value. As a result, the simulation resembles conditions encountered in systems which display self-organized criticality (SOC) [26]. These systems are characterized by a driving and a relaxation mechanism. In our studies, the increase of the radius is the driving factor that injects potential energy at various positions in the system and the conversion from potential to kinetic energy is the relaxation mechanism. The balance between the injected and dissipated energy is linked through the local Newtonian dynamics that conserves total energy. Another characteristic feature of SOC is that the system must be driven slowly. For our purposes, this translates into changing $\lambda(t)$ after sufficiently long time intervals. For a LJ potential, the driven changes in the distance scale of the inter-particle interaction amount to very large potential energy changes (figure 3(b)) that are not compatible with slowly driving the system.

As repeatedly increasing the radii is not an attractive option (because of the finite size of the simulation system), after some time we reset the system's original temperature and particle radius. If the temperature exceeds a certain threshold, the radii are rescaled to their original value ($\lambda(t) = 1$) and the velocities are rescaled so that the starting temperature is restored (figure 2). This is achieved by rescaling the velocities ($\mathbf{v}_i$) with a factor determined by the average temperature ($T_{\mathrm{avg}}$) and the average kinetic energy ($E_{\mathrm{kin,avg}}$),

$$\mathbf{v}_i \rightarrow \mathbf{v}_i \sqrt{\frac{\frac{3}{2}(N-1)k_{\mathrm{B}}T_{\mathrm{avg}}}{E_{\mathrm{kin,avg}}}}. \tag{4}$$

## 4. Results

We identify the time intervals with a varying temperature in figure 2 as non-equilibrium conditions. Now, we study the self-diffusion properties of the liquid under those non-equilibrium conditions. For a single time step, the mean, standard deviation and kurtosis of $P(\Delta x), P(\Delta y)$ and $P(\Delta z)$ are calculated. The standard deviation ($\sigma$) and kurtosis ($k$) are defined in the standard fashion,

$$\sigma(t) = \sqrt{\frac{1}{N}\sum_{i=1}^{N}(\Delta x_i(t) - \overline{\Delta x(t)})^2} \tag{5}$$

$$k(t) = \frac{\mu_4(t)}{\sigma^4(t)} - 3, \tag{6}$$

with $\mu_4$ the fourth moment about the mean. This definition ensures that for a Gaussian distribution, the kurtosis vanishes.

To normalize the width of the different distributions, the displacements are divided by the standard deviation of the distribution at this time instance. This normalization enables one to compare the $P(\Delta x/\sigma)$ that are obtained at different times. Figure 4(a) compares $P(\Delta x/\sigma)$ for a typical equilibrium time instance with one obtained at a representative non-equilibrium time instance. Under non-equilibrium conditions, the tails of $P(\Delta x/\sigma)$ are considerably heavier than under equilibrium conditions. Moreover, a higher concentration of particles in the centre of the distribution is observed. These characteristics are typical for a leptokurtic distribution. The kurtosis of the out-of-equilibrium $P(\Delta x/\sigma)$ is larger than the typical noise level under equilibrium conditions.

J. Stat. Mech. (2010) P04004

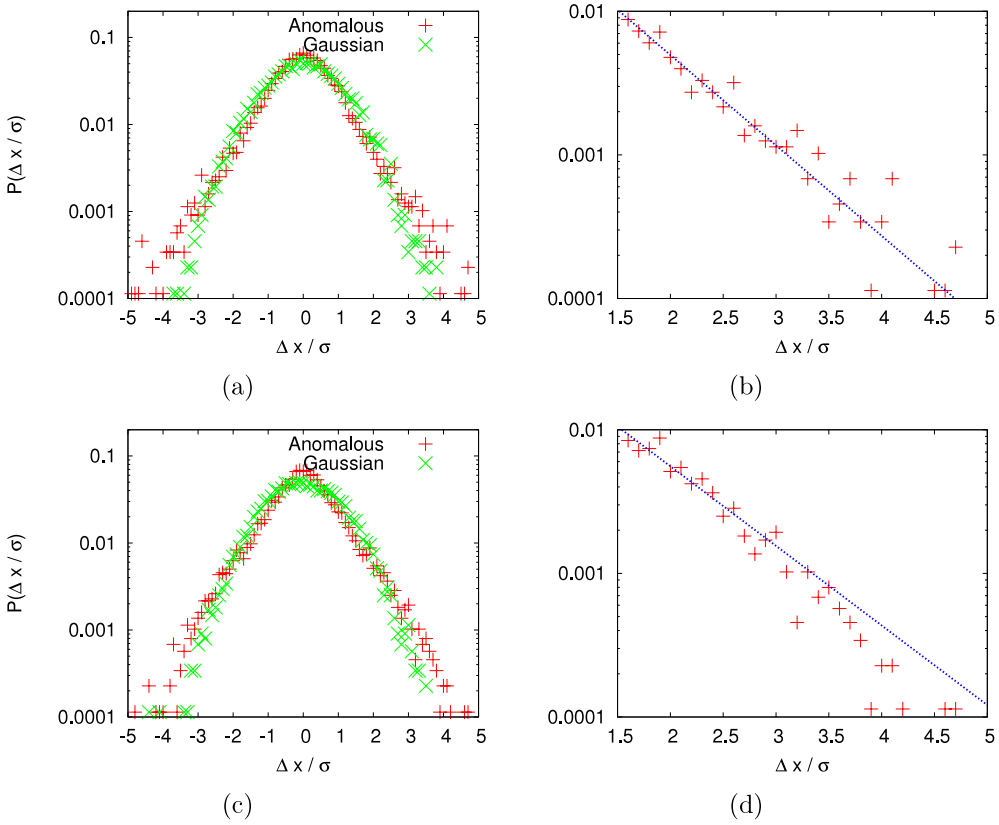


**Figure 4.** $P(\Delta x/\sigma)$ for two typical equilibrium (Gaussian) and non-equilibrium (anomalous) situations with initial density $\rho = 0.5$ and temperature $T = 0.7$. The upper panels are for $\lambda(t = 0) = 0.7$ after four rescalings. The lower panels are for $\lambda(t = 0) = 0.75$ after four rescalings. The right panels are a fit of $P(\Delta x/\sigma > 1.5)$ with (7). The best fit parameters are $a = 0.090 \pm 0.005$ and $b = 0.14 \pm 0.01$ for the upper right panel and $a = 0.072 \pm 0.006$ and $b = 0.13 \pm 0.01$ for the lower right panel.

We have found that after effectively enlarging the particles, anomalous characteristics can be found in the single-time-step displacement distributions $P(\Delta x/\sigma)$. After rescaling the interaction four times with $\lambda(t = 0) = 0.75$ and $\tau = 500$ (sufficient to reach equilibrium again), we have obtained anomalous distributions in $P(\Delta x/\sigma)$.

To establish the non-Gaussian shape of the tail of $P(\Delta x/\sigma)$ under non-equilibrium conditions, we have fitted it with an exponential because a power law is notoriously hard to observe in a sample of finite size, such as ours:

$$P\left(\frac{\Delta x}{\sigma}\right) = a \exp\left(-b\frac{\Delta x}{\sigma}\right), \qquad \left(\frac{\Delta x}{\sigma} > 1.5\right). \tag{7}$$

As can be seen in figures 4(b) and (d), the distributions are well fitted by (7). This result confirms that the $P(\Delta x/\sigma)$ have heavier tails than a Gaussian distribution.

The distributions of figures 4(a) and (c) are obtained by taking data during one time step. Summing these distributions for different time steps results in better statistics. Figure 5(a) shows the result for $P(\Delta x/\sigma)$ after summation of 50 distributions during anomalous and normal (Gaussian) simulation conditions. Remark that $(|\Delta x|/\sigma) > 4$



J. Stat. Mech. (2010) P04004

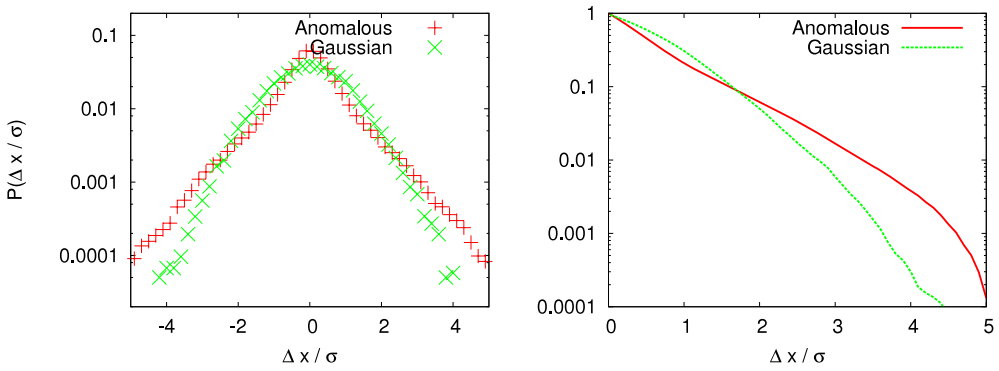


**Figure 5.** Left: normalized summation of 50 'anomalous' and 'Gaussian' distributions of $P(\Delta x/\sigma)$. Right: normalized cumulative distribution of the sum of 50 'anomalous' and 'Gaussian' distributions $P(\Delta x/\sigma)$.

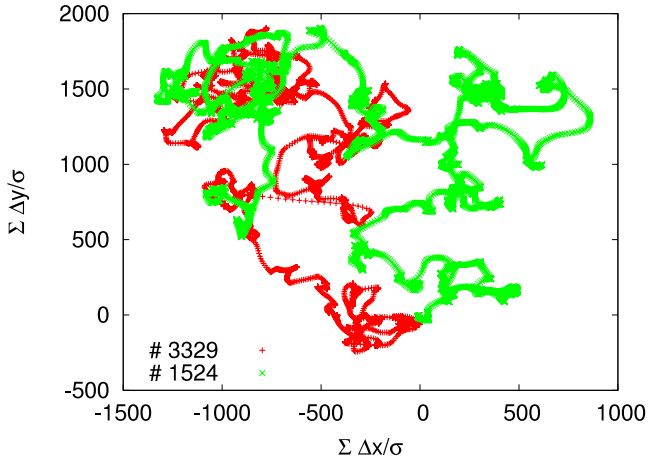


**Figure 6.** Projection on the $xy$ plane of $\sum_t \Delta r(t)/\sigma(t)$ of particles No 1524 and No 3329 during a simulation of 100 000 time steps.

events are one order of magnitude more likely under anomalous (non-equilibrium) conditions than under Gaussian (equilibrium) conditions. We find a fair amount of $5\sigma$ events and some rare $8\sigma$ events. The normalized cumulative distribution of figure 5 clearly illustrates that the self-diffusion properties of the liquid are distinctive during the non-equilibrium and equilibrium periods of the simulation. In non-equilibrium conditions, small $\Delta x/\sigma$ are more likely, medium $\Delta x/\sigma$ less likely and large $\Delta x/\sigma$ far more likely.

We now wish to study the trajectories of the individual particles during the complete simulation that alternates equilibrium with non-equilibrium conditions. To this end, we selected two particles: particle No 1524 for which $|\Delta x/\sigma|$ does not exceed 5 during the simulation (since this limit is not attainable in a Gaussian simulation regime) and particle No 3329 for which this is not the case. Figure 6 illustrates that the random character of the trajectories for both particles is maintained over the simulation time.

Figure 7 shows $\Delta x/\sigma$ as a function of time for these particles. The 'anomalous' behaviour of particle No 3329 is confined to the time period 32 000–33 000. By contrast, no anomalous behaviour is discernible in the behaviour of particle No 1524.



J. Stat. Mech. (2010) P04004

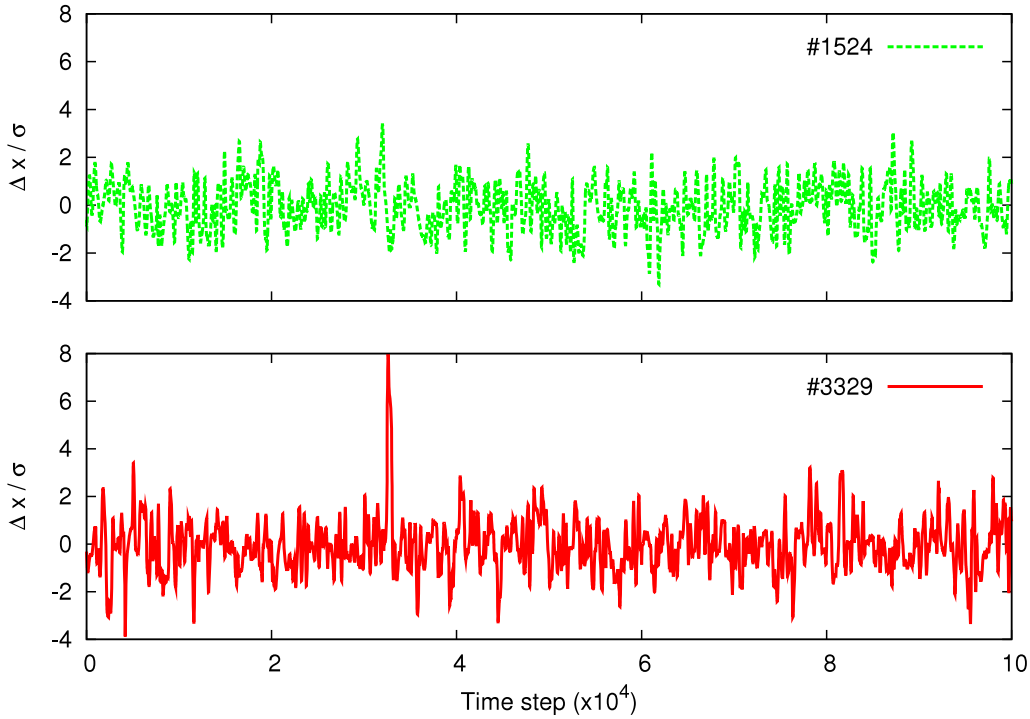


**Figure 7.** Single-time-step displacements $(\Delta x(t)/\sigma(t))$ of particles No 1524 and No 3329 during a simulation of 100 000 time steps.

To establish the robustness of our technique for generating conditions of anomalous self-diffusion in a monatomic liquid, we have investigated its dependence on the parameters of the simulations. The non-equilibrium conditions are determined by the size of the rescaling parameter $\lambda(t = 0)$ and the time intervals $\tau$ between two subsequent radial rescalings. During a simulation of 100 000 time steps, the system goes through different periods of non-equilibrium conditions. The kurtosis of $P(\Delta x/\sigma)$ is computed for every time step and the maximal kurtosis is saved for every set of parameters. In figure 8 the maximum kurtosis of the simulation is plotted as a function of $(1/\lambda(t = 0))$ and $\tau$. The parameter $\tau$ is chosen between 100 and 1500 time steps, since equilibrium is always reached after 1500 time steps. $\lambda(t = 0)$ is confined to $1 < 1/\lambda(t = 0) < 1.4$, which means that the density change in one step is limited to $1 < \Delta\rho < 2.7$. Figure 8 clearly shows that the anomalous character of $P(\Delta x/\sigma)$ remains present independently of the rescaling parameters. The time interval between two subsequent rescalings has only a minor influence on the maximal kurtosis ($k_{\max}$). The value of $\lambda(t = 0)$ adopted, on the other hand, has a larger influence on $k_{\max}$, but the anomalous characteristics are present over the entire $\lambda(t = 0)$ interval.

The influence of the parameter $\lambda(t = 0)$ on the system is further illustrated in figure 9. Although $\lambda(t = 0)$ has an influence on the height of the peak of the kurtosis during the non-equilibrium periods of the simulation, one can clearly see that the main characteristics of this non-equilibrium period remain roughly the same. In figure 9, the non-equilibrium periods all have a period of ∼200 time steps during which the kurtosis is equivalent to zero. This can be interpreted as the system requiring some time to convert the injected



J. Stat. Mech. (2010) P04004

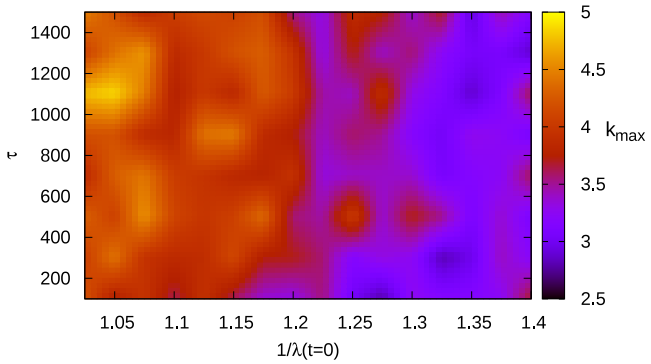


**Figure 8.** Maximal kurtosis ($k_{\max}$) of a simulation as a function of the rescaling parameter ($1/\lambda(t=0)$) and the time interval $\tau$ between two subsequent rescalings.

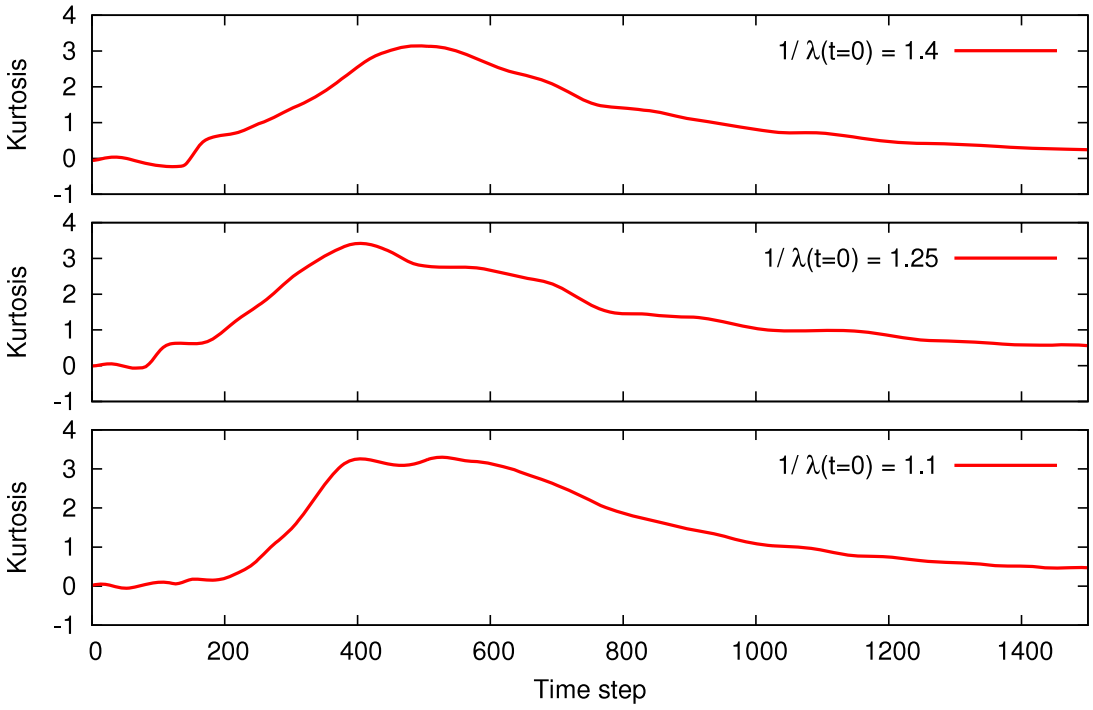


**Figure 9.** Kurtosis during a typical non-equilibrium period for three different values of $\lambda(t=0)$, with $\tau = 1500$. Time step 0 corresponds to a driven rescaling of the size of the molecules.

potential energy into kinetic energy. For $200 \lesssim t \lesssim 500$, the kurtosis features a steep ascent. For $t \gtrsim 600$, we observe a gentle decline to the equilibrium value. This reflects the fact that our simulation system has relaxed to an equilibrium situation with Gaussian self-diffusion properties.

The same robustness in the results applies to variations in the initial density and temperature of the system, provided that they generate a system in the liquid phase. The short-range order and particle mobility typical for a liquid are necessary conditions. They

J. Stat. Mech. (2010) P04004

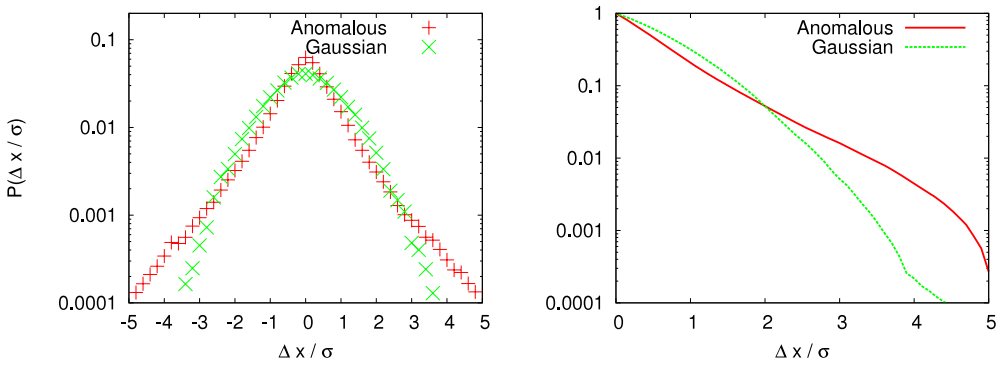


**Figure 10.** Normalized $P(\Delta x/\sigma)$ for a four-dimensional simulation with 4375 particles, summed over 350 time instances, for two typical equilibrium (Gaussian) and non-equilibrium (anomalous) situations, with $\lambda(t=0)=0.8$ and $\tau=1000$.

generate the required balance between mobility and interaction, allowing the system to dissipate the potential energy surplus after being driven.

The robustness of the anomalous character of the self-diffusion properties under non-equilibrium conditions is a very useful result. It indicates that the qualitative features of the self-diffusion properties of the system are rather insensitive to the two parameters ($\lambda(t=0)$ and $\tau$) that characterize the non-equilibrium behaviour. As a consequence, we can ascertain that it is the internal dynamics of the system that causes the non-Gaussian properties of $P(\Delta x/\sigma)$.

We have also tested the robustness of our results to changes in the potential. To this end, we have performed simulations with the following potential: a LJ form for $r_{ij} > 0.9$ and a polynomial $ar^6+b$ for $r_{ij} < 0.9$ [27]. This potential has the long-range LJ properties and a soft core. We have obtained non-Gaussian distributions almost identical to those obtained with $U_{\mathrm{SC}}(r)$.

A further test of the robustness of our technique can be made for dimensions other than 3. For two dimensions we obtain inherent anomalous self-diffusion of the system even in equilibrium conditions and with a LJ potential, as expected [5, 14]. Figure 10 shows the result of a simulation in four dimensions. We have used the same technique as was adopted for the 3D results of figure 5. From figure 10 it is clear that during the non-equilibrium time periods the self-diffusive properties are non-Gaussian. This provides further evidence for the robustness of the proposed technique.

## 5. Conclusion

In summary, we have presented a computational method, based on out-of-equilibrium MD simulations with a soft-core potential, that generates dynamical conditions of anomalous diffusion for the distribution of the one-dimensional displacements of the particles. This behaviour arises because the driving mechanism, i.e. the potential energy artificially injected into the system by increasing the radius of the particles, generates regions of increased potential energy. The dissipation of this potential energy under conditions of constant energy results in a small amount of very fast particles. For a broad range of the parameters involved, our technique generates anomalous diffusion in the simulation.



J. Stat. Mech. (2010) P04004

In this way we have created a simple and solid method for achieving anomalous self-diffusion in an interacting system. This emergence of global behaviour that cannot be determined from local properties is also a property of self-organized criticality, to which our model bears similarities. In the proposed simulation system, equilibrium circumstances correspond to single-step displacements that are confined to a certain scale $\sigma$ (Gaussian like). Upon slowly driving the system and having it dissipate locally injected bursts of potential energy, we observe displacements $\Delta x$ over a much more extended range and no characteristic size for $\Delta x$ exists any more. In other words, the single-step displacement distributions $P(\Delta x/\sigma)$ obtain heavy tails. We find that this emergent feature does not require any fine-tuning of the interaction parameters or of the driving protocol. Therefore, we consider that during the non-equilibrium simulation periods the system reaches a self-organized dynamical state. Available computer models that display self-organized criticality (e.g. sandpile models [28]) are typically characterized by two timescales. The external driving needs to be much slower than the typical timescale required for internal relaxation. The computer model that is described in this paper shares this property: between two subsequent (forced) swellings of the molecules we need to leave sufficient time for the system to relax. In order to observe the emergent behaviour of the heavy tails in the $P(\Delta x/\sigma)$ during the non-equilibrium periods we need to have a time evolution where bursts of activity are separated by relatively calm periods. Upon driving the system too fast we do not observe any general characteristic feature emerging in the $P(\Delta x/\sigma)$.

For the above-mentioned analogies, we consider that the proposed simulation system may serve as another computer method for studying self-organized criticality. Whereas there is no fundamental understanding of self-organized criticality and metastable states at the very fundamental level, it is worth pursuing its study. After all, an abundance of phenomena in economics, Earth sciences, biology and physics are characterized by phenomena that are not confined to a certain scale. At present, we are investigating whether the driven system of interacting units presented here can serve as a rough model for simulating the robust features of return distributions in financial markets.

## References


[1] Einstein A, 1905 *Ann. Phys., NY* **17** 549
[2] Lévy P, 1954 *Théorie de L'addition des Variables Aléatoires* (Paris: Gauthier-Villars)
[3] Mantegna R N, 1994 *Phys. Rev.* E **49** 4677
[4] Mantegna R N and Stanley H E, 1994 *Phys. Rev. Lett.* **73** 2946
[5] Klafter J and Sokolov I M, 2005 *Phys. World* **18** 29
[6] Bouchaud J-P and Georges A, 1990 *Phys. Rep.* **195** 127
[7] Mandelbrot B, 1963 *J. Business* **36** 394
[8] Mantegna R and Stanley H, 1995 *Nature* **376** 46
[9] Kiyono K, Struzik Z and Yamamoto Y, 2006 *Phys. Rev. Lett.* **96** 068701
[10] Ramos-Fernández G *et al*, 2004 *Behav. Ecol. Sociobiol.* **55** 223
[11] Wong I *et al*, 2004 *Phys. Rev. Lett.* **92** 178101
[12] Janes G S and Lowder R S, 1966 *Phys. Fluids* **9** 1115
[13] Takeuchi H and Okazaki K, 1996 *Mol. Simul.* **16** 59
[14] Liu B and Goree J, 2007 *Phys. Rev.* E **75** 016405
[15] Havlin S and Ben-Avraham D, 2002 *Adv. Phys.* **51** 187
[16] Schmiedeberg M and Stark H, 2006 *Phys. Rev.* E **73** 031113
[17] Juhász R, 2008 *Phys. Rev.* E **78** 066106
[18] Majda A and Kramer P, 1999 *Phys. Rep.* **314** 237
[19] Alder B and Wainwright T, 1970 *Phys. Rev.* A **1** 18
[20] Kresse G and Hafner J, 1993 *Phys. Rev.* B **47** 558


doi:10.1088/1742-5468/2010/04/P04004


J. Stat. Mech. (2010) P04004

[21] Mondello M and Grest G, 1997 *J. Chem. Phys.* **106** 9327
[22] Crozier P *et al*, 2001 *Phys. Rev. Lett.* **86** 2467
[23] Franzese G, 2007 *J. Mol. Liq.* **136** 267
[24] de Oliveira A, Franzese G, Netz P A and Barbosa M C, 2008 *J. Chem. Phys.* **128** 064901
[25] D'Orsogna M R *et al*, 2006 *Phys. Rev. Lett.* **96** 104302
[26] Bak P, 1996 *How Nature Works: The Science of Self-Organized Criticality* (New York: Copernicus)
[27] Tappura K, Lahtela-Kakkonen M and Teleman O, 2000 *J. Comput. Chem.* **21** 388
[28] Jensen H, 1998 *Self-Organized Criticality* (*Cambridge Lecture Notes in Physics*) (Cambridge: Cambridge University Press)

J. Stat. Mech. (2010) P04004